Modification of properties of reinforced concrete through nanoalumina electrokinetic treatment

Wu Hangtong[a], Torabian Isfahani Forood[b,*], Jin Weiliang[a], Xu Chen[a], Redaelli Elena[b], Bertolini Luca[b]

[a] Zhejiang University, Institute of Structural Engineering, Yuhangtang road 866, Hangzhou, China.

[b] Politecnico di Milano, Department of Chemistry, Materials and Chemical Engineering "G. Natta" Via Mancinelli 7, 20131 Milan, Italy.

[*] Corresponding author: email: forood.torabian@polimi.it, tel: +390223994732

Abstract

An attempt was made to drift nanoalumina particles into concrete pores through electrokinetic treatment. An external electric current (current density = 3 A/m^2) was applied for 3 and 15 days in reinforced concrete blocks toward steel reinforcement and microstructural characterizations (i.e. morphology observation and porosity analysis) were performed on concrete fragments of different depth from exposure surface. The morphology observation evidenced transport of nanoalumina from the exposure surface even reaching the rebar-concrete interface (up to 25-30 mm, in 15 days treatment). The porosity analysis of treated samples revealed that reduction of porosity of rebar interface was more pronounced as compared to the exposure surface and the treatment for 15 days was more beneficial for porosity refinement than treatment for 3 days. Effects of the electrokinetic NA treatment on strength of

rebar-concrete interface were evaluated through pull-out test. The results showed that by increasing current density, bond strength of rebar-concrete interface increased.

1 Introduction

Application of external electric current for prevention, protection and mitigation of corrosion of the reinforcement in reinforced concrete (RC) structures is getting more demanded, discussing durability of RC structures. Several techniques have been developed as electrochemical repair methods applying external electric current such as cathodic prevention [1] and protection [2,3], electrochemical chloride extraction (ECE) [4,5], electrochemical realkalization [6] and electroosmotic transport [7]. Other techniques such as electrokinetic nanoparticle treatment [8-10] and crack closure by electrodeposition [11,12] also have been developed but have received less attention in the literature.

Electrochemical repair methods are based on the accelerated transport of charged particles (ions, inhibitors, etc.) inside pore structure by migration mechanism, under the influence of an electric field [8]. The electric field, which is established through RC structure, can extract chloride ions toward the surface or generate alkalinity close to the cathode (rebar). Simultaneously, the electric field can cause ions or cationic corrosion inhibitors or other positively surface charged particles to drift towards reinforcement through migration mechanism during an electrochemical repair method. Cathodic inhibitors (positively charged) have been reported to be transported utilizing the conventional setup of electrochemical repair methods [13,14].

Suspended nanoalumina (NA) can be considered as formed by surface charged particles depending on pH value of the suspension and on surfactant by which the particles are modified. For instance, considering suspension of bare NA, for pH lower than 8 NA particles had positive surface charge and for pH higher than 8 the NA particles had negative surface charge [15]. Thus, transport of NA particles

into concrete pores by means of external electric field could be theoretically possible through a so-called electrokinetic treatment.

Electrical transport phenomena, which are based on the charge separation inside the electric double layer, are called in general electrokinetic [16]. Electrophoresis is a type of electrokinetic treatment and is defined as the movement of dielectric particles relative to a stationary liquid through application of an electric field. Surface charged particles induce charge separation inside the liquid phase, see Fig. 1. Electric field may propel the particles with positive zeta-potential through the liquid towards the cathode. The transport of the particles is in direct relation with zeta-potential of the particles, electric field and in inverse relation with viscosity of the fluid [17]:

$$v_\infty = -\frac{E_\infty \epsilon \xi}{\mu} \qquad (1)$$

where v_∞, E_∞, ϵ, ξ and μ are velocity of the fluid far from the particle with respect to the particle, component of electric field far from the particle along with the velocity, permittivity (F/cm), zeta-potential (V) and viscosity of the fluid (g/cm.s), respectively. As a consequence, a particle with positive zeta-potential moves in the direction of electric field.

Cardenas et al. [18] made the first attempt to drift NA coated nanosilica (NS) particle into the concrete through electrokinetic treatments. In another study, Sanchez et al. [8] modified a setup in order to conduct migration treatment of negatively charged NS into hardened mortar. One of the differences between these two studies is that Cardenas et al. [18] used nanoparticle suspension as anolyte, while Sanchez et al. [8] used nanoparticle suspension as catholyte. This transport of nanoparticles may influence porosity of hardened cement composites and as a result, may modify durability properties.

Several durability properties of cement composites have been claimed to be affected by electrokinetic transport of nanoparticles. Permeability of cement paste was reduced by 1-3 orders of magnitude by

electrokinetic treatment of NA coated NS [18]. Capillary porosity of concrete was found to be reduced with electrokinetic treatment of NS [8,9]. Cylindrical samples were treated by electrokinetic NS transport for 8 days [8] and for 4 hours [9]. The samples were immersed in water after treatment and after approximately 28 days immersion, the electrical resistivity increased with respect to that of before the treatment. Moreover, resistance to carbonation after a treatment with NS for 4 h increased with respect to untreated sample [9]. Beneficial effects of transport of nanoparticles by electric current were also reported with respect to reinforcement corrosion. A significantly lower corrosion current density was measured for electrokinetic treated (EN) concrete compared to untreated, when the concrete was re-exposed to chloride solution after ECE treatment followed by EN treatment [10]. Kupwade-Patil et al. [10] claimed that nanoparticles appeared to form a physical barrier against chloride re-penetration.

Application of plain NA suspension as anolyte in electrokinetic treatment for reinforced concrete is an innovative rehabilitation method and is not studied in the literature. In this study, reinforced concrete blocks were subjected to electrokinetic treatment with NA suspension. The aim was to investigate the feasibility of transport of NA into concrete under the action of an external electric field and to study influences of the nanoparticle transport on microstructure of the concrete. Microstructural characterization such as morphology observation and porosity analysis were conducted on samples of different depth from exposure surface. Further information was provided concerning influence of NA electrokinetic treatment and effects of application of electric current on bond strength of rebar-concrete interface through pull-out test.

2 Material and experimental methods

2.1 Materials

Ordinary portland cement was used for fabricating concrete blocks with w/c ratio 0.55. The concrete composition is presented in Table 1 and the aggregates were river siliceous particles with size in the range 0.15-9.5 mm. NA suspension was used with concentration of 20% by total mass. Density and pH values of the suspension were, respectively, 1.14 g/cm^3 and in the range of 5-7. Particle size distribution and cumulative volume fractions of the NA suspension, conducted by measurement of dynamic light scattering (DLS), are shown in Fig. 2. Based on the figure, 100% of the volume of tested NA suspension had particles finer than 10 nm.

2.2 Sample preparation

Two types of reinforced concrete specimens were fabricated and undergone electrokinetic NA treatment for: microstructural characterization (labeled as type I) and pull-out test (labeled as type II). The concrete specimens were cured for 28 days in a curing chamber with 95% relative humidity and temperature 23°C. Schematic of specimen type I is shown in Fig. 3. Two smooth carbon steel bars with diameter of 12 mm were embedded in a concrete block with dimensions of 150mm×150mm×100mm. A schematic of specimen type II is shown in Fig. 4: Cubic specimens with size of 100 mm were cast in which one smooth carbon steel bar was embedded. For type I, four specimens and for type II, eight specimens were cast. Side surfaces of the specimen were covered by epoxy resin to ensure unidirectional injection flow, as shown in Fig. 3 and 4. The steel mesh was used as anode and the steel bars were used as cathode to apply the electric field.

2.3 Test methods

Electrokinetic treatment - The specimens were put in contact with the NA suspension with depth of 1-3 mm. Details of the treatments are described in Table 2. One specimen of type I was subjected to

electrokinetic treatment of NA for 3 days and another one for 15 days, labeled as NA3 and NA15, respectively. The current density was 3 A/m^2 with respect to reinforcement surface area. Moreover, a treatment was designed by replacing the anodic electrolyte, i.e. NA suspension, with pure water and was labeled as water-treated. The aim of this specific treatment was to ensure the fact that microstructural changes after treatments are actually originating from NA transport into concrete.

Specimens of type II were initially subjected to three electrokinetic NA treatments for duration of 15 days (two specimens for each treatment) labeled as II-0.5, II-1.5 and II-3, as shown in Table 2, with different current densities (0.5, 1.5 and 3 A/m^2, respectively). After treatments, the samples were stored in the lab until the reinforcement was pulled-out, measuring load and slip between the rebar and concrete.

Microstructural characterization - After electrochemical treatments, several cores with diameter of 10 mm in the position shown in Fig. 3 were extracted for microstructural characterizations. The cores were cut to three disks with 10 mm length and labeled as: exposure surface (1st layer), intermediate layer (2nd layer) and interface layer (3rd layer), see Fig. 3. Morphology observations and porosity analysis were performed by FEF650 Scanning Electronic Microscopy from FEI Corporation and by Mercury Intrusion Porosimetry (MIP), respectively.

Pull-out test - The pull-out test was targeted at investigating effect of NA treatment on the bond strength of rebar-concrete interface. In addition, effect of increasing current density on bond strength was evaluated. The test was done with a machine carrying a maximum load of 25 kN. Displacement control mode was used in the loading process. Loading rate on rising phase was 0.2 mm/min. The decline rate after the failure was 0.1 mm/min. When the specimens relatively slipped more than 4.0 mm, loading was stopped.

3. Results and discussion

3.1 Morphology observation

3.1.1 Exposure surface

Fig. 5a shows a macropore of a fragment taken from the exposure surface (1st layer) of a sample treated with NA3. In this figure, round particles occupying fraction of the pore volume could be detected. Higher magnification of the macropore in Fig. 5b also evidenced the presence of round shape particles inside the concrete pore. These round shape particles, which could be associated with NA particles, have an average particle size of 130 nm. According to the particle size distribution of dispersed NA (section 2.1), the particles in the figure could be agglomeration of several individual NA. This agglomeration could be originated from the application of electric current as well as from sample drying process required for SEM. Fig.s 5c,d show other examples of micrographs, captured from other positions of the same fragment where bunch of NA agglomerates can be observed.

Fig. 6a shows an air void of a fragment, taken from the exposure surface (1st layer) of a sample treated with NA15. This image shows that many NA agglomerates occupied the volume of the void and reduced its total volume. Fig. 6b shows a magnified picture of a crack containing NA agglomerates with average measured particle size of 70 nm. Total volume of the crack was also reduced by the agglomerates. Fig. 6c shows an image, captured from a different position of the same fragment. It shows a bunch of NA agglomerates, accumulated inside a concrete pore. A portion of the figure is magnified and depicted in Fig. 6d, showing several NA agglomerates with similar average measured particle size to Fig. 6b (i.e. 70 nm). A high resolution image of NA agglomerates was obtained in Fig. 6d, thanks to a particularly favorable position of this portion of the fragment with respect to electron beam and detector of the microscope. NA agglomerates in the figure were characterized by rough surface rather than smooth spherical surface and the roughness had granular shape. This supports the

hypothesis that round shape particles observed at lower magnification are agglomerates of the individual NA particles.

Comparing Fig.s 6a,b with Fig.s 5a,b, the number of spherical particles that could be seen in Fig 6 for NA15 is higher than Fig. 5 for NA3. This supports the observation that longer duration of treatment for NA15 might have resulted in transport of larger number of NA particles into the concrete with respect to NA3 treatment.

3.1.2 Rebar interface

In order to study possibility of transport of NA particles into inner layers of the concrete, fragments of rebar-concrete interface layers were also observed. Fig. 7a shows a fragment taken from the steel-concrete interface (3rd layer) of samples treated with NA15. In Fig. 7b, round particles could be detected with average measured particle size finer than 100 nm. As previously shown, these particles could also be NA agglomerates. Fig. 7c,d shows other images, captured from other positions of the same fragment as Fig. 7a,b. NA agglomerates with similar measured particles size as Fig. 7b are indicated by solid arrows. A bunch of NA agglomerates could also be seen, as shown by solid arrows in Fig.7e.

The presence of agglomerates of nanoalumina particles at the steel-concrete interface, suggest that NA particles were drifted via applied electric field and reached the cathode. They might be transported up to 25-30 mm by constant current density of 3 A/m^2 during 15 days treatment. The real mechanism of the NA transport is difficult to be assessed. It might be assumed that they were moved also by the electrophoretic movement. The NA suspension had pH lower than 7 and NA particles, according to [15], are expected to possess positive surface charge. Under this condition, the driving force is expected to be oriented in the direction of the electrical field so that they could be accelerated towards the

cathode, i.e. the steel reinforcement. To confirm the results of the morphology observation, possible effects of NA transport on concrete porosity of the exposure surface and inner layers were investigated.

3.2 Porosity analysis

In order to investigate effects of NA transport on the porosity, the initial pore size distribution along the depth from the exposure surface of an untreated specimen was investigated; then the effects of electrokinetic NA treatments for the same depths were evaluated.

3.2.1 Untreated specimen

Fig. 8 shows the pore size distribution and cumulative pore volume for exposure surface (1st layer), intermediate layer (2nd layer) and interface layer (3rd layer) taken from untreated specimen. Fig. 8a shows that maximum intrusion (which is characterized by a peak having the highest dV/dlog$D$) for inner layers (2nd and 3rd) was shifted toward finer pores with respect to exposure surface. For pores smaller than 4 µm, the pore size distribution of rebar interface was approximately similar to that of the intermediate layer. Volume of pores with size 4-90 µm for rebar interface was considerably higher than in the exposure surface and intermediate layer. From Fig. 8b, the total porosity of exposure surface (13.9%) was similar to intermediate layer (13.6%). Total porosity of rebar interface was around 19% which is quite larger than two other layers.

3.2.2 Effects of NA treatment on exposure surface

Fig. 9 shows results of porosity analyses for exposure surface of specimens treated with NA3, NA15, water-treated (two cores of the same specimen) and untreated. To aid investigating effect of NA electrokinetic treatments, initially treated specimens will be compared to untreated specimen. Then, NA treated specimens will also be compared to water-treated specimens.

The pore size distribution of NA3 and NA15 showed that the maximum intrusion reduced and slightly was shifted toward smaller pore sizes as compared to untreated specimen. From Fig. 9a, the volume of

the pores with size 40-700 nm decreased after both NA treatments with respect to the untreated specimen; however, according to Fig. 9b, the cumulative volume of pores larger than 700 nm for NA treated specimens was higher than untreated specimen. The total cumulative pore volume and porosity of NA15 reduced and for NA3 increased with respect to untreated specimen. The effect of NA electrokinetic treatment on the porosity was small and could have been originated from two contributions i.e. NA transport and application of electric field through the specimen.

In order to study the second contribution, water-treated specimen is compared with untreated in Fig. 9a. When an electric field was employed, volume of pores with size of 40-700 nm clearly decreased with respect to the untreated one. Fig. 9b also shows that the total pore volume decreased. The porosity for water-treated was averagely 12.95% and was lower than 13.9% for untreated.

For NA15 treatment in Fig. 9a, pore volume of size smaller than 10 nm was clearly decreased as compared to water-treated. Considering the pore size distribution of NA suspension Fig. 2, it may be assumed that individual NA particles could occupy fraction of volume of pores with size finer than 10 nm. For pore sizes of NA15 larger than 10 nm from Fig. 9b, the pore distribution did not change with respect to water-treated samples. The total porosity of NA15 treatment was 12.38% and it was slightly lower than that of water-treated. Even though the NA particles might be transported, the effect on refinement of the overall porosity was negligible.

3.2.3 Effects of NA treatment on rebar interface

Fig. 10 shows pore size distribution and cumulative intrusion volume for rebar-concrete interface of specimens. Fig. 10a shows that for NA3 and NA15, the volume of pores larger than 4 μm decreased with respect to untreated. Moreover, volume of pores smaller than 10 nm decreased as well. Maximum intrusion for NA15 was found to be reduced compared to untreated. From Fig 10b, total porosity of NA3 slightly reduced and that of NA15 clearly reduced as compared to untreated.

Comparing water-treated with untreated in Fig. 10a, considerable reduction of pore volume, related to pores with size larger than 4 μm, was also seen. Maximum intrusion, however, for water-treated did not change with respect to untreated. Fig. 10b shows that total porosity, as well as total intrusion volume, decreased from almost 19% for untreated to averagely 15.85% for water-treated.

For NA3 in Fig. 10a, pore volume with pore size <10 nm was decreased with respect to water-treated. This could imply transport of NA into rebar interface within 3 days of treatment. Pore size distribution of pores >10 nm was quite similar to that of water-treated, taking into account repeatability of two fragments. Total porosity, as well as total intrusion volume, slightly decreased from water-treated 15.85% to 15.22% for NA3, Fig. 10b and it could be related to refinement of the pores <10 nm.

Comparing NA15 with water-treated in Fig.10a, a clear reduction of pore volume with pore size 80-350 nm and with size <10 nm was observed. In addition, slight reduction was also detected for amplitude of maximum intrusion of NA15 compared to water-treated, taking into account repeatability range of the water-treated fragments. Fig. 10b indicates that the total porosity reduced from 15.85% for water-treated to 13.33% for NA15.

Since an apparent reduction of pore distribution only was observed in rebar-concrete interface among different depth from the exposure surface, mechanism of the porosity refinement was further investigated for this zone. Extrusion cycles in Fig. 10b can provide information on the pore's type and porosity reduction mechanism. Pores may be classified according to their shape. Common shape terms include effective porosity and ink-bottle porosity, Fig. 11a,b, respectively. Effective porosity is the volume of extracted mercury, see Fig. 10b. Ink-bottle porosity is defined as difference between total volume of the pores in intrusion cycle and volume of the extracted mercury, when pressure is released. Transported NA particles could reduce the porosity through occupying volume of bigger pores, Fig. 11c, and through blocking ink-bottle pores, Fig. 11d. The pore blocking may result from obstruction of

entrance of ink-bottle porosity by nanoparticles. During the intrusion cycles, the complete interconnected pore space is filled with mercury. When the pressure is released, the mercury is sucked out of the pore space except for the ink-bottle and dead-end pores [19], for instance see Fig. 11a,b.

Due to large fragment sizes used (see section 2.3), the initial extrusion curves exhibited an increase in cumulative porosity volume in Fig. 10b with decreasing the pressure after reaching the maximum intrusion; consequently, as Moro et al. [20] suggested, differential mercury compression correction is needed. From the intrusion behavior displayed in the low pore sizes region (the high pressures), additional intrusion at decreasing pressure was corrected. Then, corrected effective porosity and ink-bottle porosity were evaluated for NA3, NA15, water-treated and untreated and were depicted in Fig. 11e. Comparing NA3 and NA15 with untreated, a clear reduction was observed in ink-bottle porosity of both NA treatments. The ink-bottle porosity also decreased for the water-treated samples in comparison with untreated. Both application of electric current and electrokinetic NA treatment tend to block the entrance of ink-bottle porosity of rebar interface.

The results of porosity analysis indicate that the application of an electric field itself resulted in a slight reduction of porosity. The results are in agreement to findings of Koleva et al. [21] who reported that DC current regime causes decrease in total porosity of concrete. The reason probably is related to physicochemical changes due to ion transport [21]. In addition, it could also originate from electrodeposition of the ions in the pore solution, thus precipitation of metallic oxides (such as potassium, sodium and calcium-based ions species) in concrete pores. In literature, precipitation of electrodeposits has been proposed as a possible reaction happening along with application of electric current through the concrete [10-12]. Chemical compounds such as $CaCO_3$ and $Mg(OH)_2$ could precipitate along with application of an electric current [12].

In order to compare effects of electrokinetic NA treatments on pore distribution along different depths from exposure surface, data related to total porosity (%) of the layers of the same core (extracted after a specific treatment e.g. NA3, NA15, water treated and untreated) are sorted versus the distance from exposure surface in Fig. 12. Each data point was considered as an average of the layer and was represented in the middle of the layer. Rebar interface of all cores was characterized by higher porosity with respect to exposure surface. Being pouring direction of fresh concrete during casting from the top in Fig. 3, the higher porosity of concrete close to rebar interface (3^{rd} layer) with respect to other two layers is probably due to bleeding, which takes place below the bars during casting. The electrokinetic NA treatment did not reduce porosity of the exposure surface with respect to untreated specimen; however the porosity of rebar interface for fragments of NA15 was quite lower than untreated. One of the reason why NA treatment influences rebar interface but not exposure surface could be a unit volume of interface region may contain more cement paste than exposure surface. The NA transport takes place in the cement paste, thus probability of presence of NA particles in this zone is higher than exposure surface. Another reason could be nanoparticles cannot go beyond the steel surface and thus accumulate there. The production of hydroxyl ions in the zone near the rebar, due to cathodic reaction at cathode (reinforcement), may also influence the transport of NA particles.

Considering the porosity reduction of water-treated with respect to untreated for rebar interface as compared to the correspondent reduction for exposure surface, the reduction was more severe for rebar interface than exposure surface. Similarly, Koleva et al. [21] reported that the application of the electric current in concrete caused lower porosity in zone close to cathode as compared to the zone close to anode. They believed that ion transport into the zone close to cathode could be the reason of the lower porosity of this zone. In addition, production of hydroxyl ions in the zone close to rebar could promote reduction of the porosity.

3.3 Pull-out test

Pull-out test was designed for further study the effects of NA treatment for 15 days on the rebar interface. Also effects of increasing current density on bond strength were investigated. Typical load-slip curves of treatments with different current densities, as an example, are shown in Fig. 13. As it can be seen, the maximum load of the specimens treated with NA was remarkably higher than that of untreated. Table 3 summarizes average values of the maximum load and their variation, in addition to their variation (in percentage) with respect to control. The maximum load was converted to bond strength. The bond strength increased when the applied current density of the treatment increased from 0.5 to 3 A/m^2. The bond strength was noticeably improved by 70% with respect to control after NA treatment with current density of 0.5 A/m^2. Increasing current density to 1.5 A/m^2, the enhancement reached 94% with respect to control. Further increase in current density did not result in further increase of bond strength. The enhancement of II-3 was 98% (Table 3) and it was quite similar to that of II-1.5. One factor influencing bond strength is porosity of rebar-concrete interface. Thus, the reduction of the porosity of the interface could contribute to this noticeable increase. Two phenomena may occur simultaneously through application of NA treatment. On one hand, higher current density theoretically should result in higher transport of NA into concrete, as stated in section 1. So, the bond strength is expected to increase. On the other hand, overprotection of impressed current from steel mesh (anode) to steel rebar (cathode) may result in accumulation of alkali ions (K^+, Na^+, Ca^{2+} and etc.) at the rebar-concrete interface, thus softening of the C-S-H gel [21-27] and it will cause the bond strength to decrease. Some other researchers [27-30] also found that cathodic current decreases rebar-concrete interface strength, although the extent of reduction observed has been variable [22]. In total by increasing the current density, growth of the bond strength decreased.

3.4 Effectiveness of electrokinetic NA treatment

Application of electric current through RC structures may also induce another electrokinetic phenomenon so-called electroosmotic flow [7]. Electroosmotic flow of water (pore solution) in concrete pores and electrophoretic movement of NA particles could theoretically happen simultaneously during electrokinetic NA treatment due to application of electric field through the concrete. According to Bertolini et al. [7], electroosmotic flow for alkaline mortar was low and occurred in the opposite direction i.e. towards anode, as compared to that of carbonated mortar that occurred towards cathode. Assuming similar principles for electrokinetic NA treatment, one may expect simultaneous electroosmotic flow of pore water towards anode (steel mesh in this case) occurs along with electrokinetic movement of the NA particles towards reinforcement (or cathode); however, apparently electrokinetic movement of NA was dominant in this treatment, since transport of NA was evidenced by the results obtained in section 3. In agreement to these explanations, Cardenas et al. [18] also believed that in order to have sufficient transport of the nanoparticles through electrokinetic movement, it is essential for nanoparticles to move fast enough to overcome (electroosmotic) flow of water in opposite direction. It is worth mentioning that the electroosmotic flow (if it occurs) would be so little because the concrete block was not fully saturated with water or was not in contact with water; thus displaced water would not be compensated by further water and quantity of water susceptible to move under action of electroosmosis is low.

From a practical point of view, results presented in this work suggest that electrokinetic NA treatment can hardly be used as a surface treatment to build a barrier against ingress of aggressive substances, even though a slight reduction of the porosity in exposure surface was observed by NA15 treatment, see section 3.2.2. Nevertheless, this treatment could be employed simultaneously with an electrochemical repair treatment for mechanical strengthening of the rebar-concrete interface bond.

Regarding current density and duration of application of electrokinetic NA treatment, the experimental results revealed that 3 A/m^2 for 15 days exhibited the best performance in porosity reduction and bond strengthening. Current density of this technique seems to be higher than that of ECE and realkalization method. As for available data in the literature for electrokinetic treatment of nanoparticles, for instance, Kupwade-Patil et al. [10] established 1 A/m^2 for duration for 6 weeks, which in comparison to only 2 weeks duration of application of electrokinetic NA treatment is quite longer. The duration of application of this technique is also shorter than ECE method. So, application of current density as high as 3 A/m^2 for such a short period seems to be tolerable for practical applications.

4 Conclusions

An application of nanoalumina suspension as anolyte for electrokinetic treatment of reinforced concrete was developed in this study. The aim was to verify transport of the nanoalumina and to improve the microstructure of the hardened cement in the concrete cover.

NA agglomerates were observed in fragments of exposure surface and rebar-concrete interface. The porosity analysis showed that nanoalumina transport refined porosity distribution of the rebar interface, while its effect on porosity of exposure surface was small. Thus the treatment does not appear to be useful to improve the surface resistance to penetration of aggressive agents. Nevertheless the treatment for 15 days and current density of 3 A/m^2 reduced porosity of rebar-concrete interface and the treatment for 3 days caused minor reduction. Utilizing electrokinetic NA treatment for 15 days and current density up to 1.5 A/m^2, the bond strength of rebar-concrete interface considerably increased with respect to untreated samples. Further increase of the current density to 3 A/m^2 did not result in further enhancement of the bond strength.

Acknowledgements

The authors would like to acknowledge the financial support of the European Union Research Council by way of grant no. FP7-PEOPLE-2011-IRSES, the National Natural Science Foundation of PR China by way of grant no. 51408534, no. 51578490 and no. 51278459, the Natural Science Foundation of Zhejiang Province by grant no. LQ14E080010.

References

[1] Pedeferri P. Cathodic protection and cathodic prevention. Constr Build Mater, 1996;10:391-402.

[2] Bertolini L, Bolzoni F, Pastore, T, Pedeferri, P. Cathodic protection of reinforcement in carbonated concrete. J. Appl. Electrochem, 1998;28:1321-1331.

[3] Lambert, P. Cathodic protection of reinforced concrete. Anti-Corros Method M, 1995;42(4): 4-5.

[4] Drewett J, Broomfield J. An introduction to electrochemical rehabilitation techniques. Corrosion prevention association, technical notes No. 2, (Hampshire, UK, May 2011), pp. 8.

[5] Mietz, J. Electrochemical rehabilitation methods for reinforced concrete structures-state of art report. EFC No. 24, institute of materials communication, London, UK, 1998, pp. 57.

[6] Redaelli E, Bertolini L. Electrochemical repair techniques in carbonated concrete. Part I: electrochemical realkalization. J Appl Electrochem, 2011;41:817–827.

[7] Bertolini L, Coppola L, Gastaldi M, Redaelli E. Electroosmotic transport in porous construction materials and dehumidification of masonry. Constr Build Mater, 2009;23:254–263.

[8] Sánchez M, Alonso M.C, González R. Preliminary attempt of hardened mortar sealing by colloidal nanosilica migration. Constr Build Mater, 2014;66:306–312.

[9] Fajardo G., Arquímedes CL, Dulce CM, Valdez P, Torres G, Zanella R. Innovative application of silicon nanoparticles (SN): Improvement of the barrier effect in hardened Portland cement-based materials. Constr Build Mater, 2015;76:158–167.

[10] Kupwade-Patil K, Cardenas HE, Gordon K, Lee LS. Corrosion mitigation in reinforced concrete beams via nanoparticle treatment. ACI Mater J, 2012;109(6):617-626.

[11] Hasaki H, Yokoda M. Repair method of marine reinforced concrete by electrodeposition technique. Proceeding of the annual conference of Japanese concrete institute,1992;849-854.

[12] Ryu JS, Otsuki N. Crack closure of reinforced concrete by electrodeposition technique. Cem Concr Res, 2002;32:159-164.

[13] Sawada S, Page CL, Page MM. Electrochemical injection of organic inhibitors into concrete. Corros Sci; 2005;47:2063–78.

[14] Liu YJ, Shi XM. Electrochemical chloride extraction and electrochemical injection of corrosion inhibitors on concrete: state of the knowledge. Corros Rev, 2009;27:53–81.

[15] Shin YJ, Su CC, Shen YH. Dispersion of aqueous nano-sized alumina suspensions using cationic polyelectrolyte. Mater Res Bull, 2006;41:1964–1971.

[16] Aligizaki KK. Mechanism of ions transport in cement-based materials during the application of corrosion mitigating electrical techniques. Nace international corrosion conference & expo, NACE-2012-1542.

[17] Newman JS. Electrochemical systems. Englewood Cliffs, NJ: Prentice Hall; 1973.

[18] Cárdenas HE, Struble LJ. Electrokinetic nanoparticle treatment of hardened cement paste for reduction of permeability. J Mater Civil Eng, 2006;18:554–60..

[19] Quercia G, Spiesz P, Hüsken G, Brouwers HJH. SCC modification by use of amorphous nanosilica. Cem Concr Compos, 2014;45:69–81.

[20] Moro F, Bohni H. Ink-bottle effect in mercury intrusion porosimetry of cement-based materials. J. Colloid Interface Sci. 2002;246:135-149.

[21] Koleva DA, Copuroglu O, van Breugel K, Yea G, de Wit JHW. Electrical resistivity and microstructural properties of concrete materials in conditions of current flow. Cem Concr Compos, 2008;30:731–744

[22] Page CL. Interfacial effects of electrochemical protection methods applied to steel in chloride-containing concrete. Rehabilitation of concrete structures. Proceeding of RILEM international conference, 1992;179-188.

[23] Bertolini L,Yu SW, Page CL. Effects of electrochemical chloride extraction on chemical and mechanical properties of hydrated cement paste. Adv Cem Res, 1996;8(31):93-100.

[24] Page CL, Yu SW, Potential effects of electrochemical desalination of concrete on alkali-silica reaction. Mag Concrete Res, 1995;47(170):23-31.

[25] Ali MG. Cathodic protection current accelerates alkali–silica reaction. ACI Mater. J. 1993;90(3):247– 252.

[26] Locke CE, Dehghanian C, Gibbs L. Effect of impressed current on bond strength between steel rebar and concrete. NACE Corrosion 83, Materials Performance and Corrosion Conference, Anaheim, 1983; 178/1–178/16.

[27] Rasheeduzzafar, Ali MG, Al-Sulaimani GJ, Degradation of bond between reinforcing steel and concrete due to cathodic protection current. ACI Mater J, 1993;90(1):8– 15.

[28] Chang JJ. A study of the bond degradation of rebar due to cathodic protection current. Cem Concr Res, 2002;32:657–663.

[29] Ihekwaba NM., Hope BB., Hansson CM. Pull-out and bond degradation of steel rebars in ECE concrete. Cem Concr Res, 1996;26(2):267– 282.

[30] Chang JJ., Yeih W., Huang R. Degradation of the bond strength between rebar and concrete due to the impressed cathodic current. J Mar Sci Tech, 1999;7(2):89– 93.

Table 1 Composition of concrete mixtures.

Design strength class	Composition (kg/m^3)			
	Water	Cement	Fine aggregate	Coarse aggregate
C30	220	406	643	1049

Table 2 Details of the treatments.

Designation	Sample type	Number of specimens	Current density (A/m^2)	Anodic electrolyte	Duration of the test (d)
untreated	I	1	-	-	-
NA3	I	1	3	nano-alumina	3
NA15	I	1	3	nano-alumina	15
Water-treated	I	1	3	water	15
Control	II	2	-	-	-
II-0.5	II	2	0.5	nano-alumina	15
II-1.5	II	2	1.5	nano-alumina	15
II-3	II	2	3	nano-alumina	15

Table 3 Average values of maximum load during pull-out test, their variation and corresponding bond strength for specimens treated with NA for 15 days and different current densities. The enhancement of bond strength with respect to reference is indicated in the parenthesis.

Specimen	Current density (A/m^2)	Average maximum load (N) and its variation	Average bond strength (MPa)
Control	-	4715±650	1.3
II-0.5	0.5	8021±220	2.1 (70%)
II-1.5	1.5	9128±1950	2.4 (94%)
II-3	3	9321±1502	2.5 (98%)

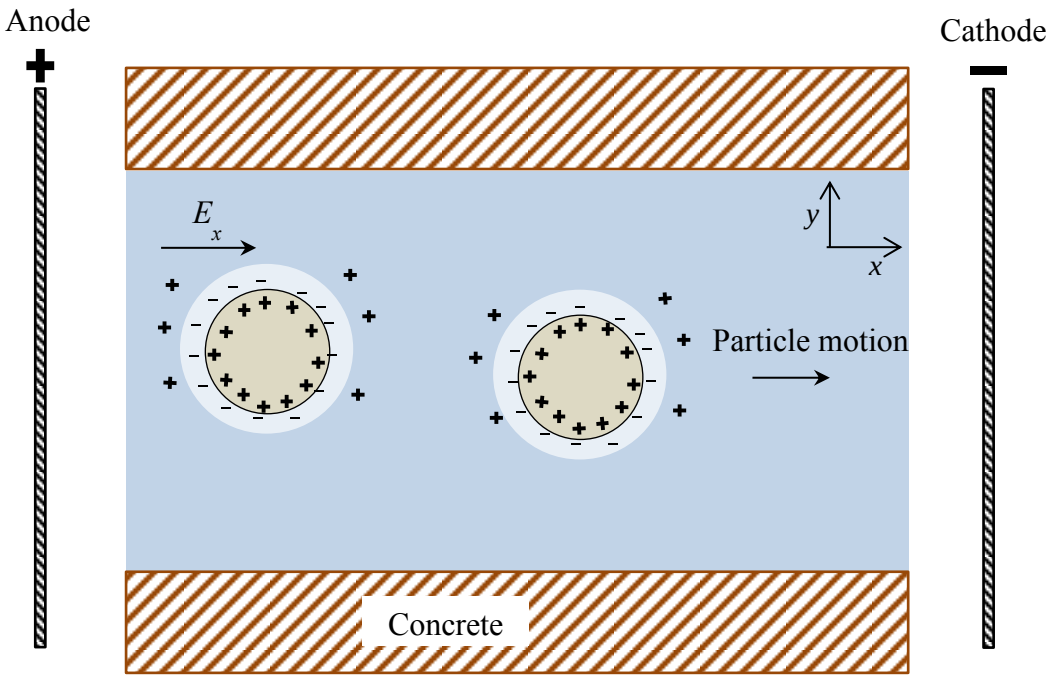

Fig. 1 Schematic of capillary porosity of concrete containing electrolyte (pore solution) and nanoalumina. Electrophoretic movement of particles with positive surface charge and charge separation around the particles is shown

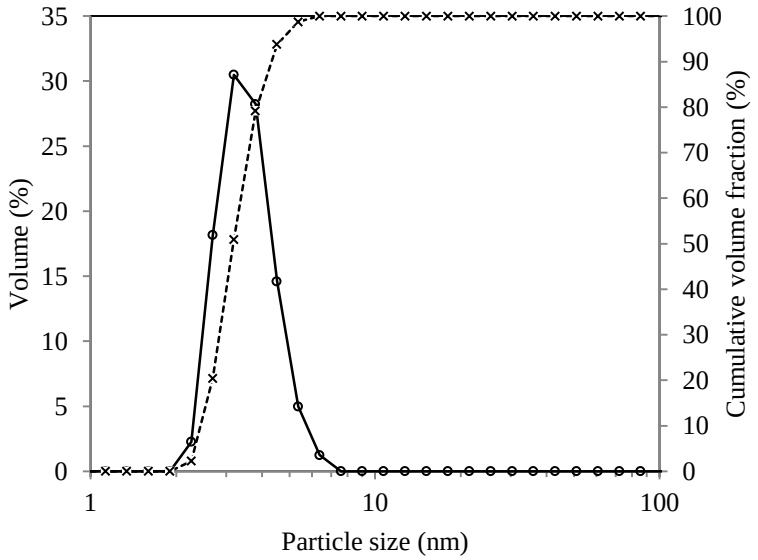

Fig. 2 Particle size distribution of NA suspension by dynamic light scattering method.

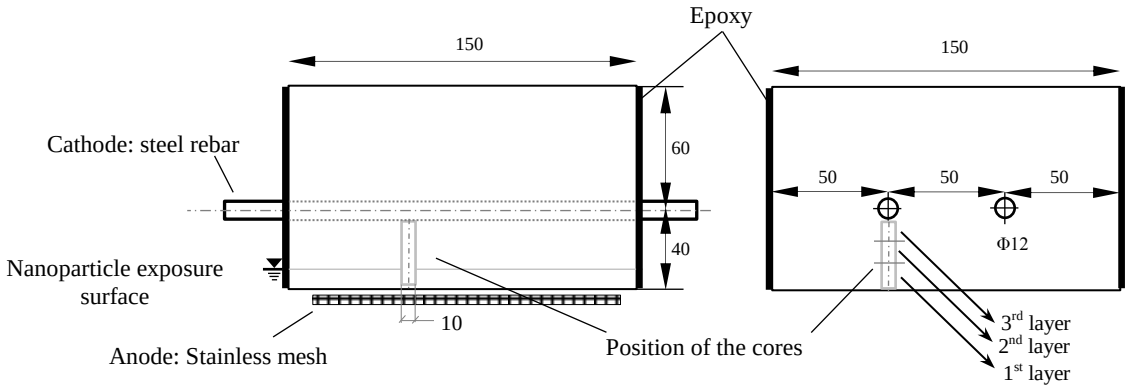

Fig. 3 Concrete block schematic of type (I) specimen. The values are in mm.

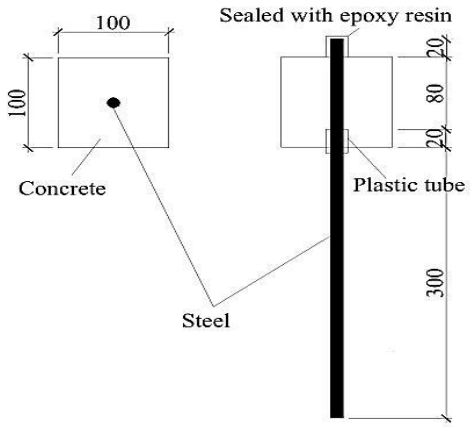

Fig. 4 Concrete cube schematic of specimen type (II). The values are in mm.

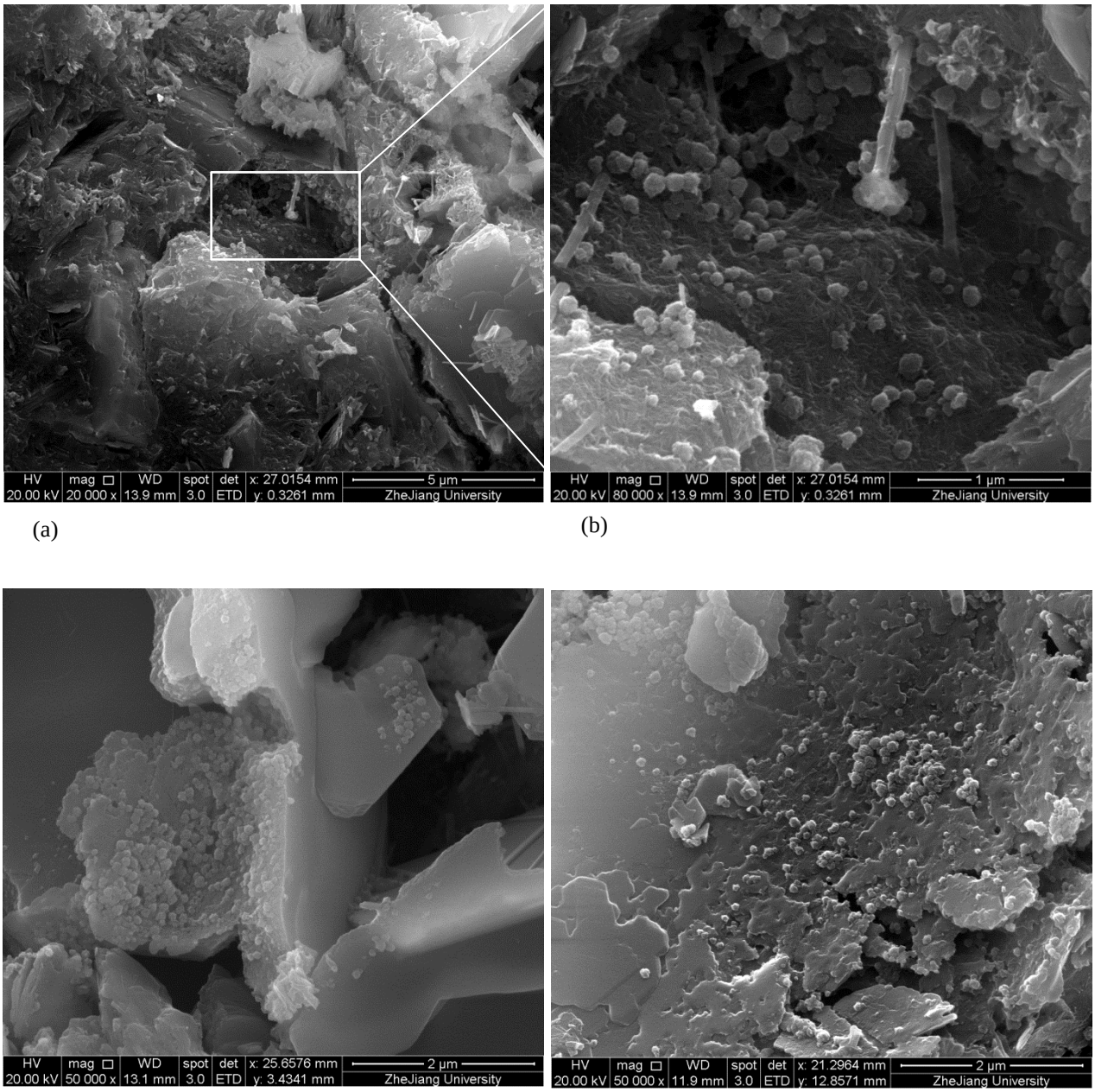

Fig. 5 SEM micrographs of fragment of exposure surface of specimens treated with NA3. (a) shows a macropore and (b) shows a magnified micrograph of the pore containing NA agglomerates with measured average particle size of 130 nm. (c,d) also show bunches of NA agglomerates.

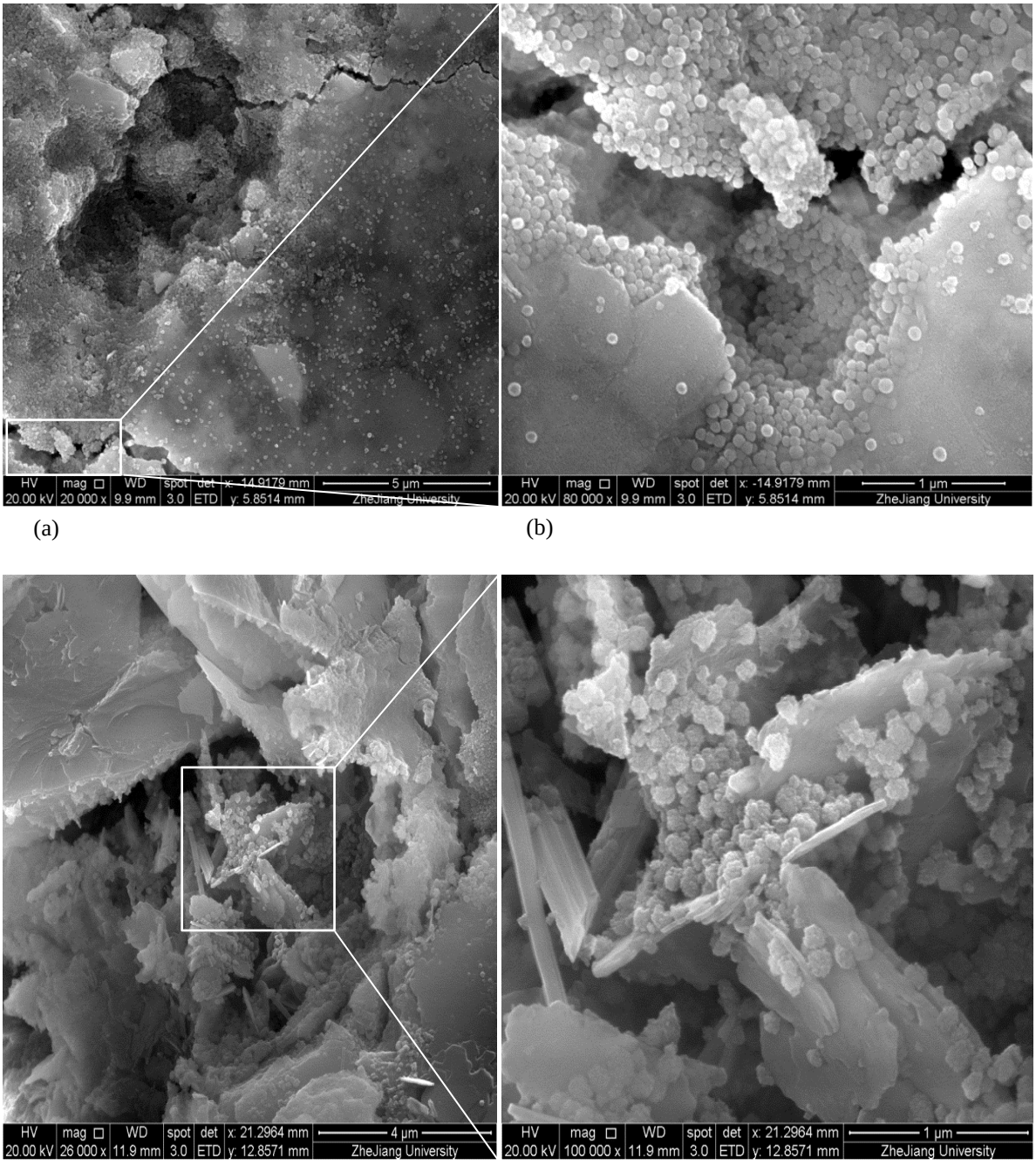

Fig. 6 SEM micrographs of fragments taken from exposure surface (1st layer) of specimen treated with NA15. (a) shows an air void containing NA agglomerates. (b) shows a magnified image of a crack containing NA agglomerates with measured average particle size of 70 nm. (c) shows another micrograph of the same sample. (b) shows a magnified image of NA agglomerates with measured particle size of 70 nm.

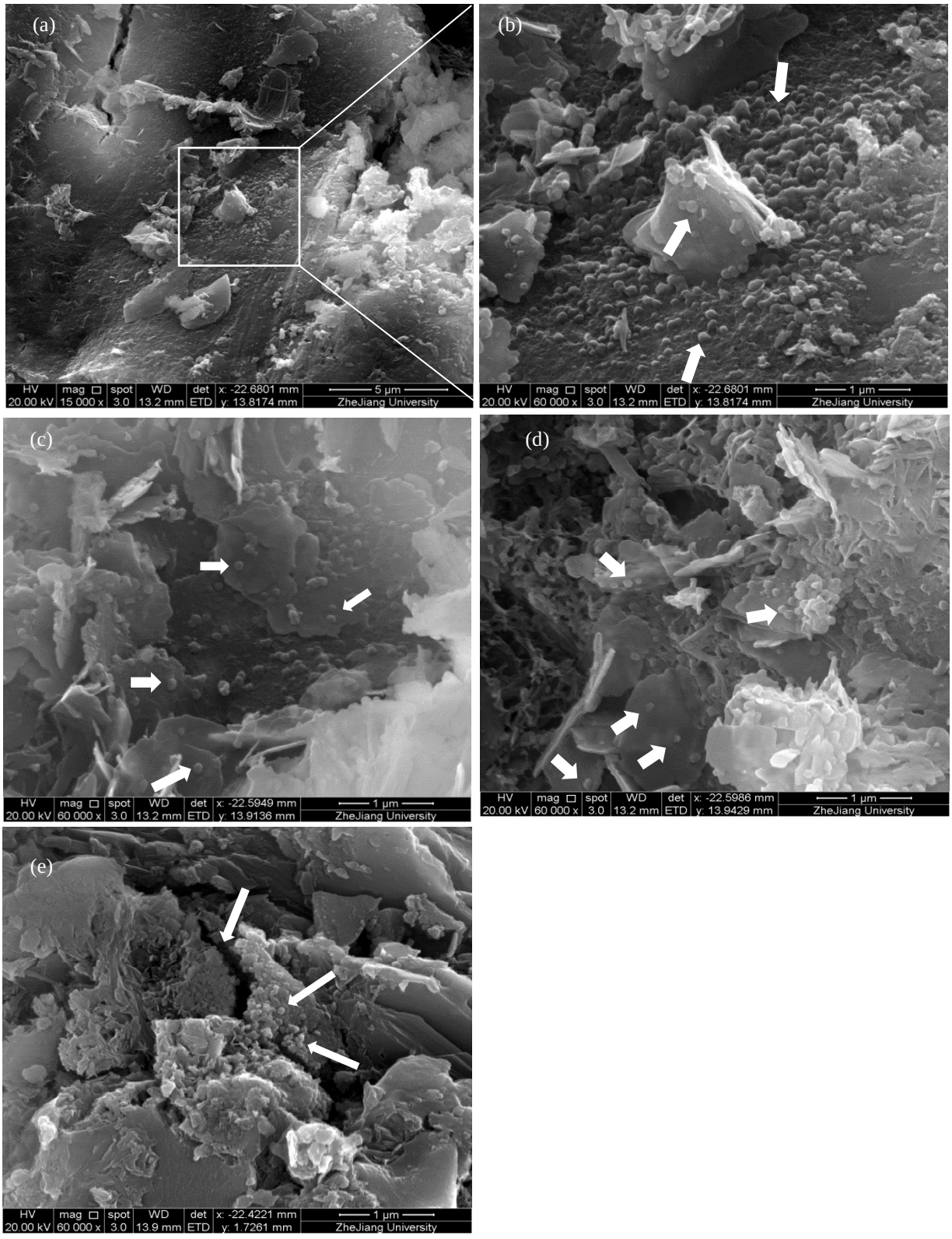

Fig. 7 (a) SEM micrographs of fragments taken from interface layer (3rd layer) of specimen treated with NA15; (b,c,d) magnified image of NA agglomerates from the same fragment and (e) cluster of NA agglomerates.

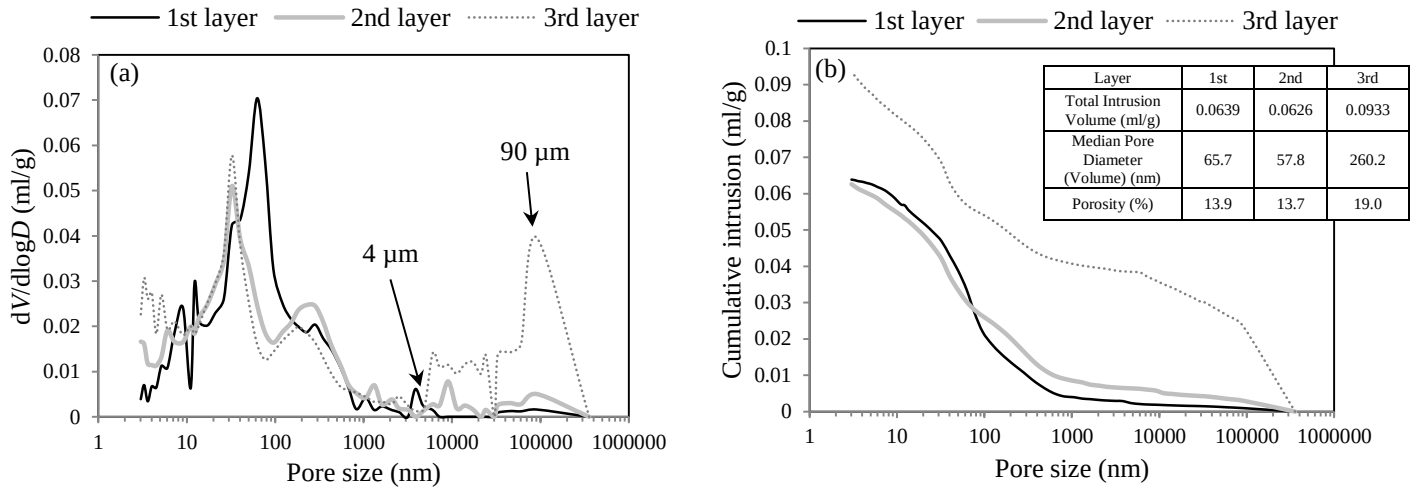

Fig. 8 (a) Pore size distribution and (b) cumulative intrusion volume for untreated specimen and different layers: 1st (exposure surface), 2nd (intermediate layer) and 3rd (rebar interface).

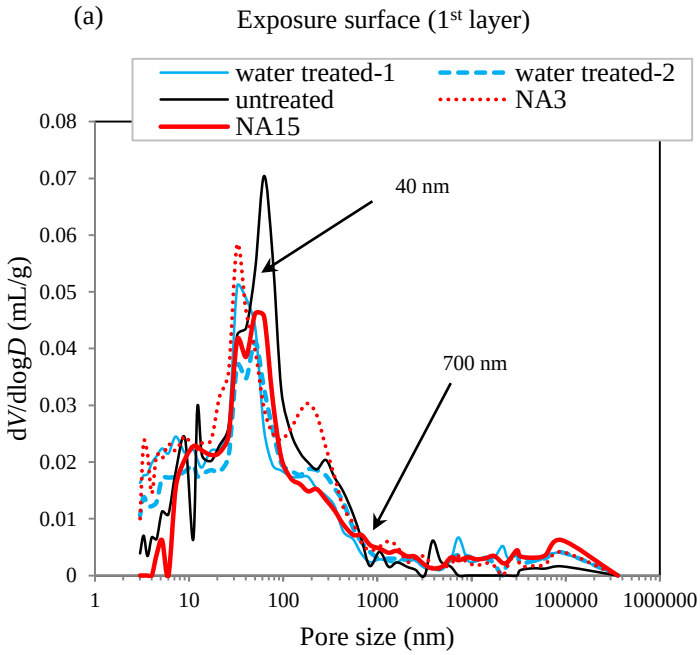

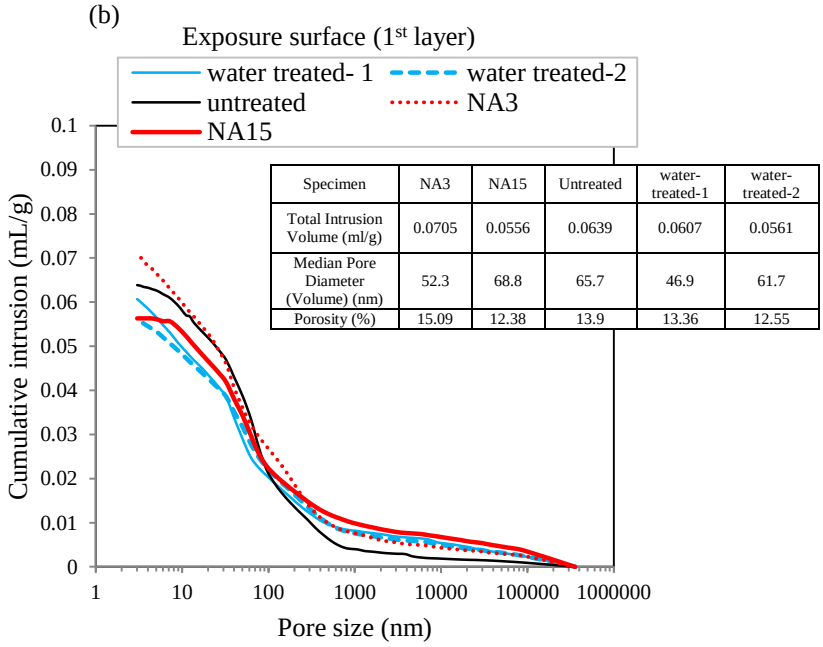

Specimen	NA3	NA15	Untreated	water-treated-1	water-treated-2
Total Intrusion Volume (ml/g)	0.0705	0.0556	0.0639	0.0607	0.0561
Median Pore Diameter (Volume) (nm)	52.3	68.8	65.7	46.9	61.7
Porosity (%)	15.09	12.38	13.9	13.36	12.55

Fig. 9 (a) Pore size distribution and (b) cumulative intrusion volume of exposure surface (1st layer) of samples: water-treated (two fragments), NA treated for 3 days and 15 days compared to untreated specimen.

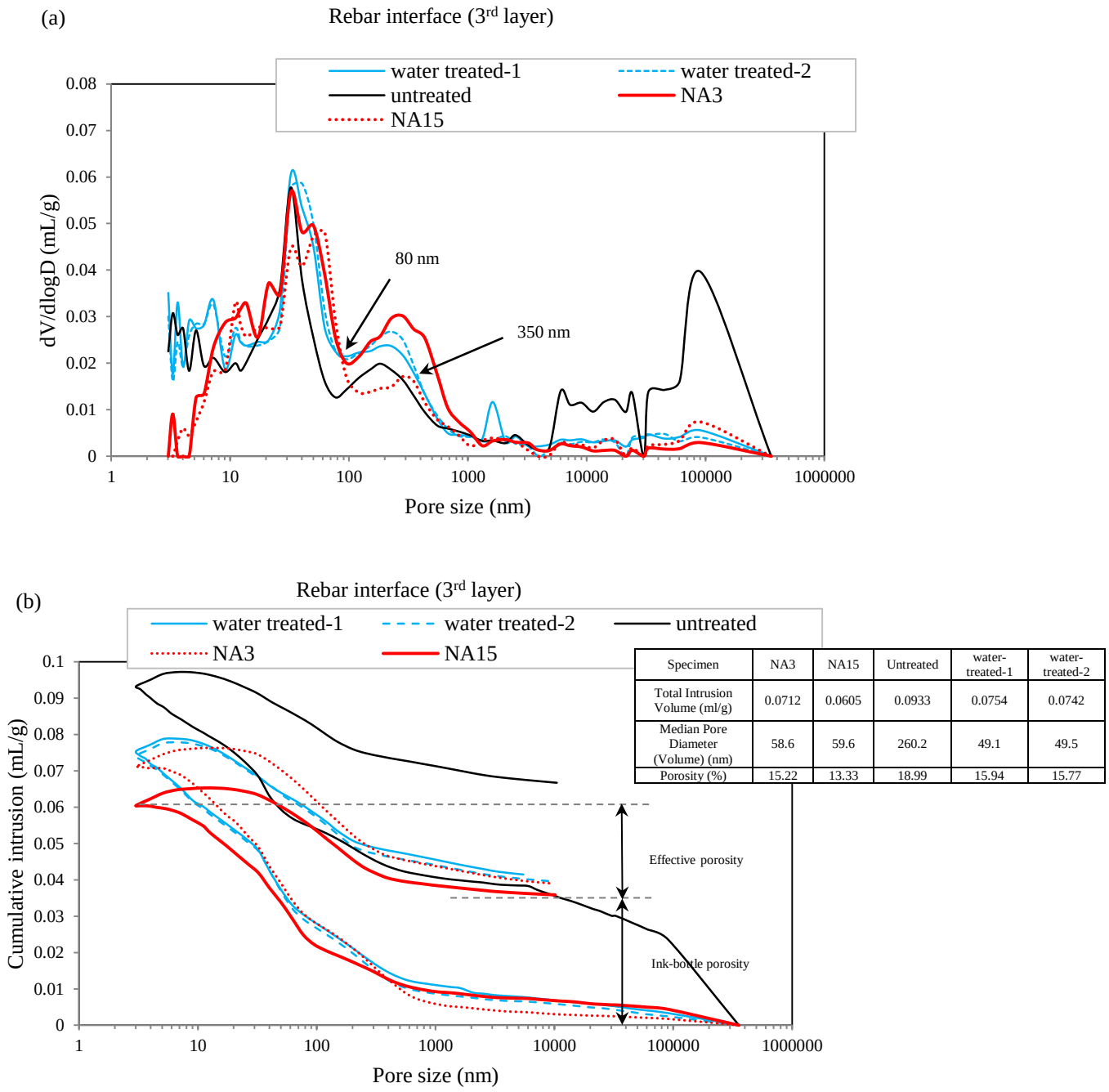

Specimen	NA3	NA15	Untreated	water-treated-1	water-treated-2
Total Intrusion Volume (ml/g)	0.0712	0.0605	0.0933	0.0754	0.0742
Median Pore Diameter (Volume) (nm)	58.6	59.6	260.2	49.1	49.5
Porosity (%)	15.22	13.33	18.99	15.94	15.77

Fig. 10 (a) Pore size distribution and (b) cumulative intrusion volume of rebar interface (3rd layer) of samples: NA treated for 3 days and 15 days, water-treated (two fragments) and untreated. Extrusion cycles are also depicted for all specimens and effective porosity and ink-bottle porosity are also indicated for NA15.

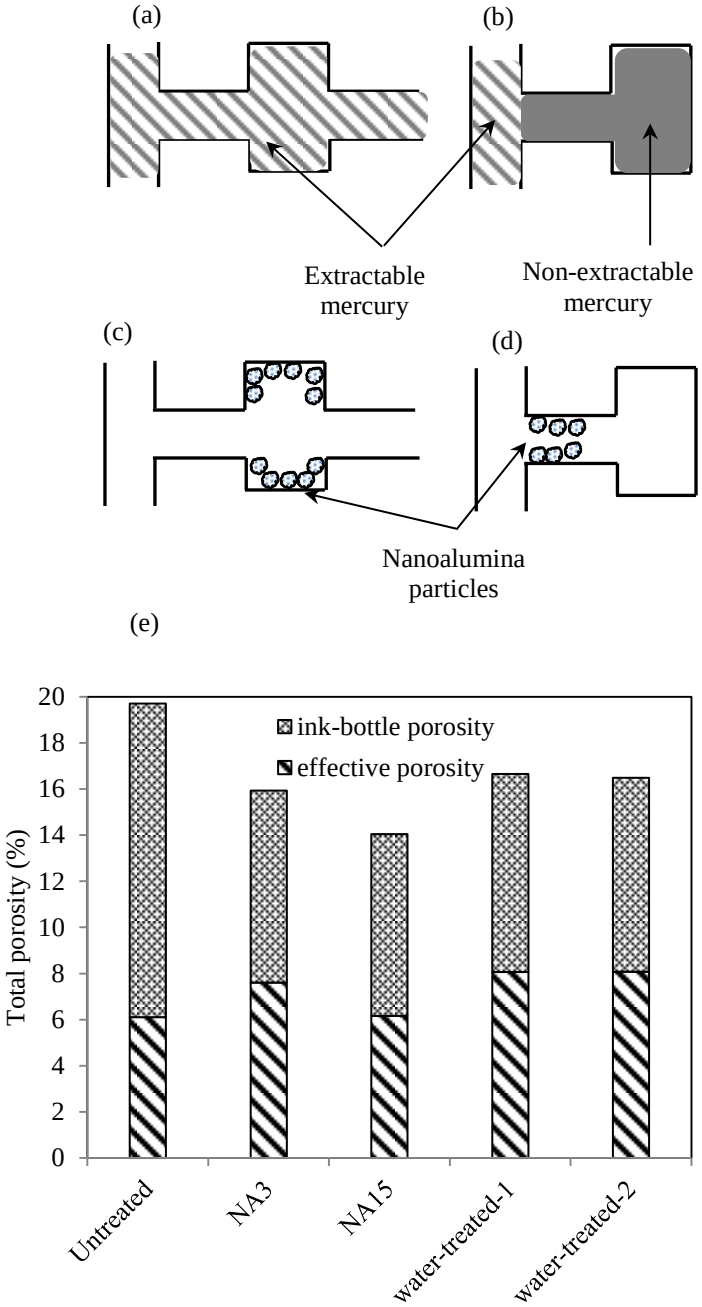

Fig. 11 Extractable and non-extractable mercury during extrusion cycle: (a) effective porosity, (b) ink-bottle porosity. Porosity reduction mechanisms by transported NA particles for (c) volume reduction of effective porosity (pore volume reduction) and (d) pore blocking of ink-bottle porosity. (e) Fractions of porosity, corrected for differential mercury compression, types according to extrusion cycle.

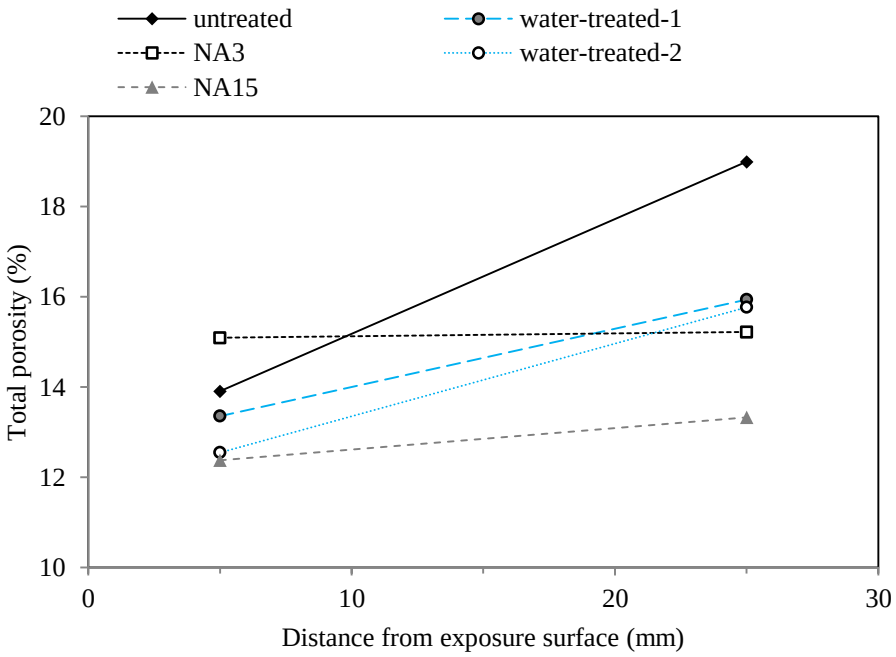

Fig. 12 Total porosity (%) measured by MIP for different layers: exposure surface, intermediate and rebar interface; for treatments: NA3, NA15, water-treated (2 fragments) and untreated.

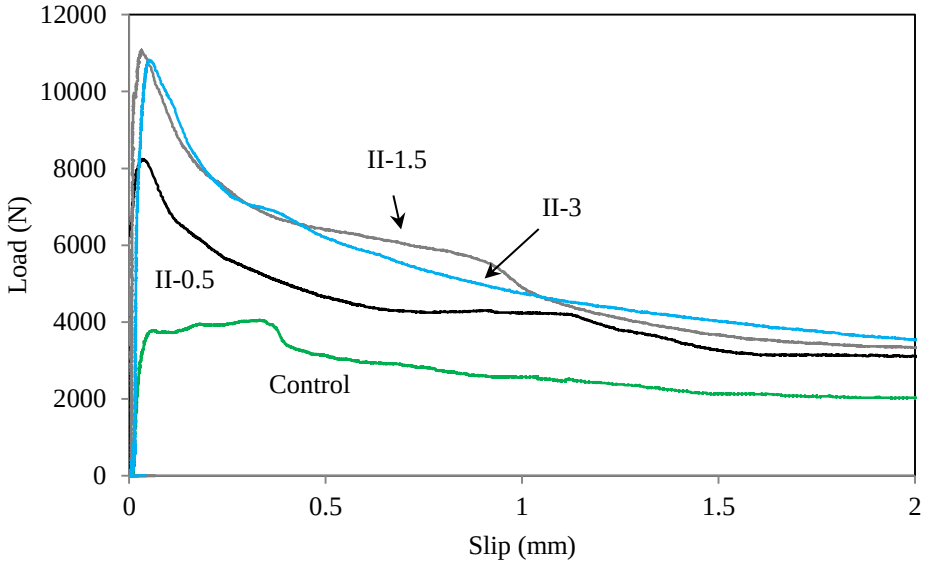

Fig. 13 Typical load-slip graphs of specimens treated with NA for 15 days and different current densities.